EXAMENSARBETE INOM TEKNIK,
GRUNDNIVÅ, 15 HP

STOCKHOLM, SVERIGE 2020

Conceptual design and construction of a UAV wing structure

SELMA RAHMAN

ANUJAN RANGANATHAN

KTH
SKOLAN FÖR TEKNIKVETENSKAP

Conceptual design and construction of a UAV wing structure

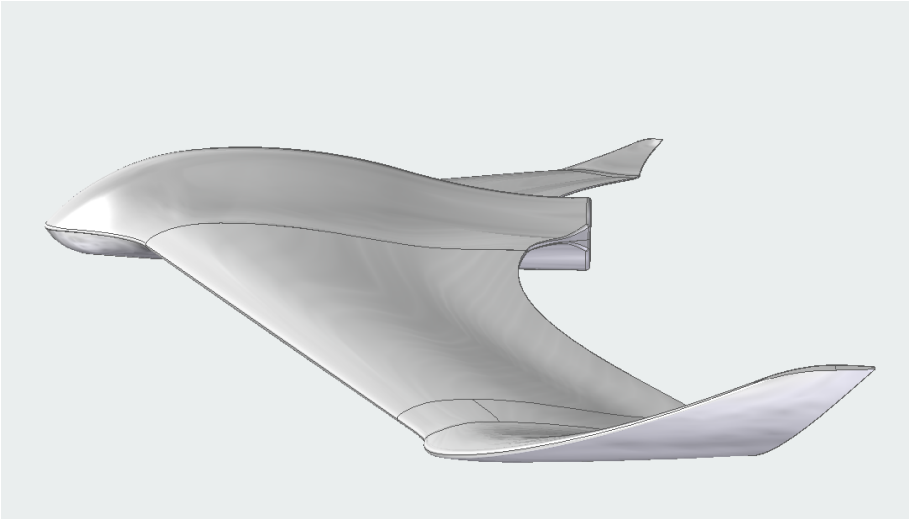

By
Selma Rahman
Anujan Ranganathan

Bachelor's thesis at SCI KTH
Supervisor: Raffaello Mariani

May 31, 2020

Acknowledgments

First off, we would like to thank the entire bachelor thesis project group, for the discussions we have had and the sharing of knowledge relevant to this project.

Secondly, Per Wennhage for answering our questions regard the relevant materials.

We would also like to thank Vivek J Shah and Mattias Olausson for guiding us through STAR CCM+ and discussing different aerodynamic topics.

Last but not least our, supervisor Raffaello Mariani for the helpful discussions we have had regarding the project.

Abstract

This report presents the design of the wing structure for a UAV called Skywalker X8. A model of the UAV was given and analyzed to design a wing box structure that is twice the size of the current model, with "greener" technology and lightweight materials. The loads that act upon the UAV were simulated and thereafter analyzed with the help of the CFD program called Star CCM+. Modifications on the CAD model and the FEM simulations were performed in Siemens NX. Eight different combinations were tested from the following five materials: CFRP (carbon fiber reinforced polymer), LDPE (low density polyethylene), polyethylene, polypropylene, and balsa wood. The results that best fit the requirements given was the combination of polypropylene as the wing skin and balsa as the honeycomb structure. This design weighed 3.576 kg and had the following stresses: 0.671 MPa, 0.340 MPa, 1 MPa, and 4 MPa for the angle of attacks at 1,2,3, and 6 degrees respectively. A modification of the trailing edge, which was the implementation of a Gurney flap, was made to see if it improved the lift-to-drag ratio, but unfortunately it did not so it was not developed further.

Sammanfattning

Denna rapport kommer att presentera en design och konstruktion av höger vinge på en drönar-modell (UAV), X8 Skywalker. CAD modellen var given och användes vid de aerodynamiska och hållfasthets simuleringarna. Syftet med projektet var att konstruera vingen utifrån dessa perspektiv för vingen i fördubblad storlek, med "grön" teknik i åtanke. Belastningarna som verkar på drönaren beräknades med hjälp av ett program, Star CCM+, som behandlar CFD-simuleringar. Redigering av CAD modellen och FEM-analyserna utfördes med hjälp av Siemens NX. Åtta olika kombinationer av 5 olika material testades, vilket är de följande: CFRP (carbon fibre reinforced polymer), LDPE (low density polyethylene), polyeten, polypropylen och balsa. Resultaten som uppfyller kraven bäst var polypropylen som vingens ytterhölje och balsa som honeycomb-strukturen. Denna konstruktion vägde totalt 3.576 kg och hade följande von Mises spänningar: 0.671 MPa, 0.340 MPa, 1 MPa och 4 MPa för angreppsvinklarna 1, 2, 3 respektive 6 grader. En modifiering av trailing edge gjordes för att se om det gav en förbättring av lift-to-drag ratio. Då den inte gav en önskad förändring så utvecklades den inte vidare.

Contents

Introduction

1.1 Background

As society grows more and more global, the demand for transportation across the world has increased. Today, the fastest way to transport both people and goods, from one country to another, is by aviation. As the industry has tried to keep up with the growing demand for air transportation, its carbon footprint has increased over the years.

Therefore, efforts have been made to lower the footprint of aeronautics as a whole. In recent years, the industry has tried to implement the idea of "greener" technology, meaning great emphasis has been placed on optimizing the different systems for their respective purposes (Jianyue, 2017). One major goal is to reduce the fuel consumption, which points towards the refinement of the aerodynamic performances by optimizing the shapes and surfaces of the aircraft, improving the efficiency of propulsion systems, proposing alternative energy sources, and lowering the weight of the aircraft by using lightweight materials.

Some real-life examples that consider these aspects are the Boeing 787: with being the first model in the world that is constructed out of 50% composite material and 20% aluminum (John Teresko, 2007). Boeing 787 consumes 20% less fuel than its replaced aircraft i.e Boeing 767, according to Boeing company reports (Tamar Wilner, 2011). Airbus A350 XWB is also mainly made out of carbon fiber-reinforced polymer: 53% CFRP and 19% aluminum (Airbus, 2017). An example of where the aerodynamic aspects have been tweaked is the recently introduced Boeing 777X with new composite wings and folding winglets (Boeing, 2017).

In addition to the demand for "greener" technology has fueled innovative solutions and approaches for new aircraft configurations and designs. Great focus has been placed on blended wing body designs and high aspect-ratio wings, or in other words: an aircraft with long, narrow wings blending into the body, which also becomes a lifting surface. Localized improvements on existing airframe have also been made, which is the foundation for this study.

1.2 Problem and project description

This project will focus on designing different systems of an aircraft, for a 2x scaled-up version of a given UAV model giving it a wingspan of 4 meters, concerning "greener" technology. Since the actual airfoil of the X8 Skywalker is unknown, an airfoil (MH49) was given and encouraged to use if needed. Since it was decided not to apply this given airfoil as the CAD model was given, the base for all of the simulations was done with the help of the given CAD model. This report is going to focus on designing one of these components: the wing box structure.

1.3 Purpose and goal

The goal of this project was to design and construct a CAD model of a wing box structure that is lightweight, with appropriate materials applied, so that the given specifications and requirements are fulfilled.

1.4 Methodology

The methodology for this project was roughly established right after the project descriptions were announced. However, it was later modified as the limitations and level of difficulty became more and more clear.

The methodology that was followed through, went as accordingly: after the literature review, the design of the structure was established. This design was then constructed in a CAD (computer-aided design) program and thereafter a CFD (computational fluid dynamics) simulation was performed for obtaining the maximum values of the lift and drag forces. Afterward, a FEM (finite element method) analysis was done to find the optimal material for the structure in question. Lastly, the combination of materials that best fit the requirements were chosen.

1.5 Limitations and required specification

As the X8 Skywalker model was given, the actual airfoil and wing shape were fixed with no changes allowed. The operations modes that were considered were the cruising mode with a speed of 100 km/h at an altitude of 2000 meters (this would be considered the most extreme case) while take-off and landing, acceleration, and turning the UAV around were not taken into account. Any extra load (other than pressure and maximum take-off weight) was not taken into account.

Flight mode

- Cruising speed: Maximum 100 km/h ($\approx$ 27.778 m/s)
- Maximum altitude: 2000 meters (above sea level)

Productions requirements

- Greener technology and reducing the carbon footprint
- Lightweight structure, minimizing the self-weight, and generating a good lift-to-drag ratio.

Theory

See Appendix A1 for terminology and definitions.

2.1 Aircraft aerodynamics

The most important factor for an aircraft to fly is generating lift, which is achieved when there is an uneven distribution of air pressure around the wing: lower pressure above the wing and higher pressure underneath the wing. For an aircraft to lift from the ground, this pressure distribution needs to generate a force that is greater than the total weight. To attain an increased lift force, the angle of attack must be considered, as it correlates to the lift force (to better understand what the angle of attack is, visualization of it is found in Appendix A.1). For a cambered airfoil, there will be a positive net lift at 0°, unlike symmetrical airfoils. With an angle of attack at 1° to 3° and above, the air pressure distribution will be uneven, causing a net lift. However, with the increase of the lift force and the angle of attack, the drag force increases as well. The drag force, also known as the air resistance, is the component of the aerodynamic force parallel to the chord. This component force restricts the lift of the aircraft, which leads to increased consumption of the fuel. It is therefore important to find an optimal ratio between the lift and drag force, to obtain an efficient aircraft. An ideal lift-to-drag ratio would be when the quotient is maximized: higher lift relative to drag which results in a minimized fuel consumption.

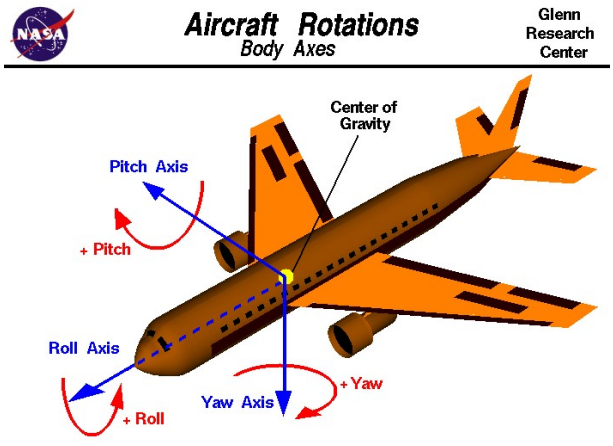

Figure 2.1: Aircraft axis (Nasa, 2015)

When doing the simulations and calculations, the coordinate system of the aircraft has to be taken into consideration. A different type of coordinate system, the so-called aircraft axis system, is implemented when doing CFD and FEM simulations. The z-axis (yaw axis), will be pointed downwards from the plane, the x-axis (roll axis) will be pointed towards the cockpit, and the y-axis (pitch axis) will be pointed towards the right-wing, which can be seen in figure 2.1.

2.1.1 The concept of air speed

As earlier stated, the lift force is a force composed of an aerodynamic force. An aerodynamic force is generated when an object is moving through a fluid or when the fluid is moving past the object, depending on which reference frame is chosen. Aerodynamic lift depends on the square of the velocity between the object and the air, according to the following formula:

$$L = \frac{C_L \rho v^2 S_1}{2} \tag{2.1}$$

where C_L is the lift constant and S_1 the reference area. Even though equation 2.1 states that the lift is correlated to the velocity, the same concept can be applied for the drag force, meaning the drag force is also dependant on the velocity.

The importance of relative velocities and a reference point are vital, since not only does the object move through the air, but the air itself has a velocity as well which needs to be taken into account. The different relative velocities are: *wind speed, ground speed* and *air spreed*. If the reference point is set as the ground below, the *ground speed* will then be the speed the aircraft moves with, relative to the ground. *Wind speed* is the speed the air moves with relative to the ground. Lastly, *air speed* is the difference between ground speed and wind speed. The relationship between ground, wind, and airspeed enables real-life experiments, like a wind tunnel test, to take place. In a wind tunnel test, the object i.e an airfoil or a wing is fixed to the walls of the tunnel, which means that the ground speed is zero and the airspeed is equal to the wind speed that is generated but acts in the opposite direction. The resulting forces acting on the object will be the same, whether the object is thought to be moving through the air or if the air is moving past the object (Nasa, 2015, b). This concept was implemented when the fluid dynamics simulations were calculated.

Aircraft ascending to a certain altitude will feel the force of gravity and the atmospheric pressure. After ascending, it will keep on flying in a given cruising speed.

The UAV will, therefore, be met by the free stream velocity which will create a boundary condition. The cruising speed has been given which will be at 100 km/h (27.778 m/s) at an altitude of 2000m. When performing the CFD simulations, the wind speed can be estimated to be around 100km/h and the aircraft wing will be the stationary object (air will move past the wing). This will create a boundary condition that can be simulated. To determine the type of flow that will be generated, the Reynolds number needs to be calculated with the following formula:

$$Re = \frac{Wind\ speed\ \cdot\ chord\ length}{kinematic\ viscosity\ of\ air} = \frac{Vc}{\nu} = \frac{27.778\ m/s\ \cdot\ 960\ mm}{1.48 \cdot 10^{-5}\ kg/(m \cdot s)} \approx 1.644 \cdot 10^{6} \tag{2.2}$$

where the kinematic viscosity is at 15° (Engineersedge, accessed 2020). A thumb rule that is commonly used when looking at the type of flow in a boundary condition is the following:

$$\begin{aligned} Re < 5 \cdot 10^5 &\implies \text{laminar flow} \\ Re > 5 \cdot 10^5 &\implies \text{turbulent flow} \end{aligned} \tag{2.3}$$

From equation 2.2 and 2.3, it can be assumed that the flow is turbulent. At this altitude and speed, the flow can be assumed to be incompressible, giving it a constant density. The incompressibility can be verified by calculating the Mach number, with the following formula ($a = 343 m/s$):

$$M = \frac{Object\ speed}{Speed\ of\ sound\ in\ air} = \frac{V}{a} = \frac{27.778\ m/s}{343\ m/s} \approx 0.081 \tag{2.4}$$

Looking at equation 2.4, since the Mach number $M << 1$ (Nasa, 2019), the flow is subsonic, as assumed.

2.1.2 Airfoil aerodynamics

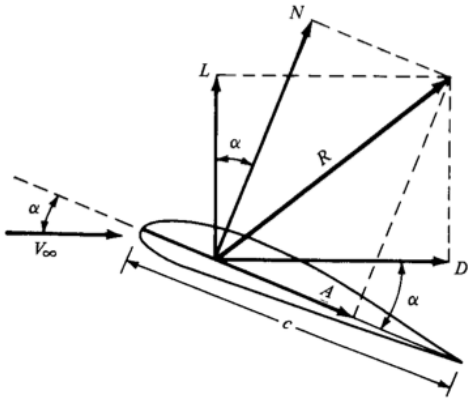

Figure 2.2: A general model of an airfoil with the main quantities (Physics Stackchange, 2013)

When designing a wing, the wing cross-section, or the airfoil, plays a major role in how efficiently it will distribute the pressure and lift. In wind tunnel testing, the airfoil is placed in the tunnel as the aerodynamic object and a stream of air is generated upstream of the airfoil. When the air is passing over the airfoil, the streamlines will be divided and change the pressure around the body. When applying an angle of attack, the free stream will divide the pressure unevenly, generating a resulting aerodynamic force (R), which consists of two components: lift (L) and drag (D) force as shown in Figure 2.2. Changing the angle of attack will give different lift and drag forces, which can thereby be mapped out in two different graphs: a lift curve and a drag curve. It is the lift-to-drag ratio, which is achieved when dividing the lift with the drag force, that is used to describe the efficiency of the airfoil in question. In aerodynamics, it is often preferred to work with dimensionless coefficients instead of e.g forces. The lift and drag forces, therefore, has corresponding coefficients, which are defined as the following:

$$C_L = \frac{2L}{\rho u^2 S_1}, \quad C_D = \frac{2D}{\rho u^2 S_2} \tag{2.5}$$

where: L is the lift force, D is the drag force, ρ is the mass density of the fluid (air), u is the flow speed of the object relative to the fluid (air), S_i is the reference area: the lower surface area of the wing for the lift coefficient and the upper surface area of the wing for the drag coefficient. The efficiency of the airfoil can be described with the help of the lift-to-drag ratio, which is defined as the lift coefficient (force) divided by the drag coefficient (force). The higher the ratio, the higher lift will be generated by the airfoil, in comparison to drag.

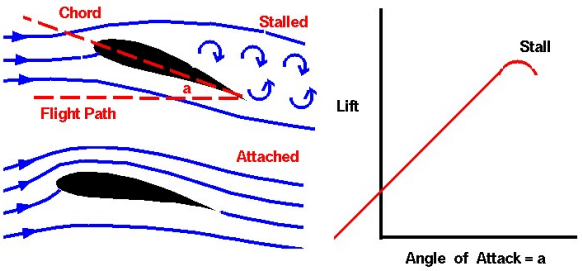

Figure 2.3: A typical graph of the lift force

For each airfoil, there will be a flow separation at a certain angle of attack which is followed by a stall, or a loss of lift. The stall can be seen in a graph where the the inclination of the curve is decreased and its highest point (see Figure 2.3). In other words, maximum lift is achieved prior to the stall.

2.2 The anatomy of an aircraft

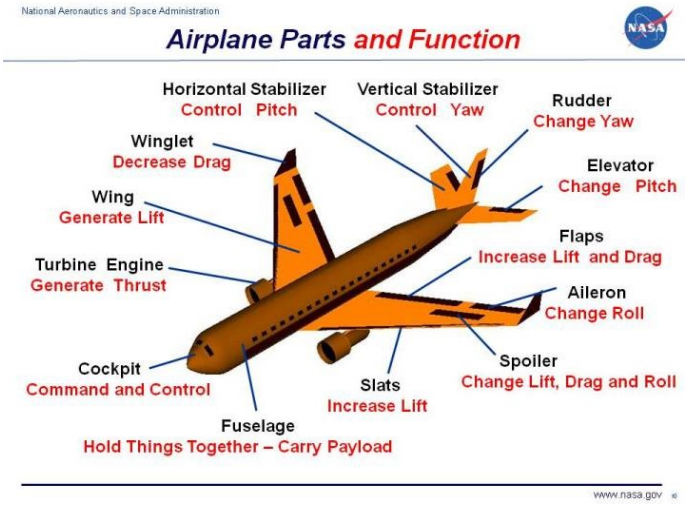

Figure 2.4: Main parts of an aircraft and their purpose (Nasa, 2015)

Aircraft comprise of many different parts which each holds specific characteristics that enhance the flight mechanism, which can be seen in Figure 2.4. There are many types of aircraft and thereby, many variations of designs each fulfill optimized for different specifications. The five parts that are mainly focused on for this UAV design, is the wing structure, trailing edge technology, leading-edge technology, propulsion, and winglet. For these five areas, many different models can be considered, each with their advantages and disadvantages.

2.2.1 Wing configuration

Aircraft wings are the essential components for flying. Many different wing types can be used for aircraft for different purposes. They can be broken down into 9 different types and they are the following: Rectangular, elliptical, tapered, delta, trapezoidal, ogive, swept-back, forward-swept, and variable sweep (Aircraftcompare, 2019). A newer design of wing configuration for UAV is the one that Boeing X-48B has: a blended wing-body. According to NASA: "*The BWB airframe merges efficient high-lift wings with a wide airfoil-shaped body, allowing the entire aircraft to generate lift and minimize drag. This shape helps to increase fuel economy and creates larger payload (cargo or passenger) areas in the central body portion of the aircraft*" (Allen, 2008). In this project, the X8 Skywalker model that was given has a wing configuration that is a cross-breed of a blended wing-body with the wings slightly swept backward.

2.2.2 Wing structure

Aside from the shape and configuration of the wing, the structure inside needs to be taken into account as well when designing wings. The purpose of the wing structure is to increase the solid mechanics of the wing and making the wing more rigid. The structure inside the wing will help to distribute the load evenly, so the stresses will not peak in some areas. The designs used for the wing structures all vary in weight, shape, size, material, and structure. The wings of an aircraft are supported through the inside, with the assistance of the wing skin. The most commonly used and widely accepted structure is the use of spars (rods along the wing) and ribs (structures across the wing). This specific structural design can vary a lot since numerous combinations can be accomplished when it comes to the number and shape of the spars and ribs and the materials applied to each component (Aircraftsystemstech, accessed 2020).

The wing spars are the fundamental support that increases the wing's strength. They extend along the full half span, which is from the wing root to the wingtip. To attach the spars to the fuselage, wing fittings, plain beams, or trusses can be used. The wing spars can be made out of wood, metals, or composite materials depending on the structural requirements for the aircraft. When making spars out of wood, four different cross-sectional configurations can be applied: solid, box, partly hollowed box, and I-shaped. When making spars out of metal it is common to use I-shaped cross-sectional configurations, however, the I-shape itself can vary in thickness or if it is hollow or not. There are also false spars that can be implemented if necessary.

They do not extend throughout the whole wing but can still be used as a hinge point for control surfaces (Aircraftsystemstech, accessed 2020).

The wing ribs are used as supporting pillars which transfer the loads from the wing skin and stringers to the spars. They extend from the leading edge of the aircraft to the trailing edge and they take the shape of the cross-section of the wing. The wing ribs are usually made out of wood or metal but specifically made out of metal if metal spars are used. As the ribs are placed laterally across the wing, they can be strengthened by the use of tapes that are woven above and below the rib sections (Aircraftsystemstech, accessed 2020).

In general, three different designs can be used with the help of ribs and spars. The first type is the mono spar design. This includes the use of one longitudinal spar together with bulkheads and ribs. It is uncommon to use one main longitudinal spar, so incorporating false spars into the design supports the structure. The second type is the multi-spar design. This incorporates the use of 3 or more longitudinal spars together with ribs and bulkheads for more contour. The third type is the box beam design. This design will take in 2 longitudinal spars and connect the bulkheads to form a contour and provide additional strength. Corrugated sheets or longitudinal stiffeners can be implemented between the box beam and the outer skin for improvement of the wings tension and compression loads (Aircraftsystemstech, accessed 2020).

2.2.3 Wing skin

The forces that act on the wing act on the wing skin first. The wing skin is a crucial component of the whole wing structure. The wing skin can be made from various materials such as wood, fabric, aluminum, or composites with varying thickness. A typical form that is used on the skin is integrating a honeycomb structure between two layers of skin, thickening the wing on the outside. It can be comprised of either a rectangular shape or a triangular shape. The most commonly used form would be just thickening the skin itself, by using the desired thickness with the desired material (Aircraftsystemstech, accessed 2020).

To increase the lift and drag forces, modifications of the leading and trailing edge can be done to increase or decrease the lift and or drag. In commercial aircraft, there are controllable flaps implemented on the trailing edge (or slats on the leading edge) that can be regulated during flight, to adjust lift and drag (see Figure 2.4).

Another modification that can be done along the trailing edge, is to design for example a Gurney flap. The Gurney flap consists of a strip of an extruded material, angled (extended wing skin), or folded sheet material which can be faced upward or downward. The flap increases the maximum lift and decreases the angle of attack at zero lift, however, it also increases the drag force. The precise dimensions, meaning the exact fraction of the chord length need to be obtained to acquire the desired and full functionality of the Gurney flap, which is generally $1 - 2\%$ of the chord length. The flap will generate vortices similar to the von Kármán vortex street but will be deflected downstream upward/downward depending on how the flap is mounted, contributing as an extra "push" when the wing is moving through the air (Gudmundsson, 2014).

2.2.4 Winglet

The design of the wingtips, or the winglets, has an impact on the aerodynamic performance of the aircraft as well. The purpose of the winglets is, to reduce the drag and increase the lift-to-drag ratio. The idea of the winglet is to hinder the high pressured air from beneath to travel to the low pressured air above the wing by creating vortices that are more controlled and smaller. The vortices created by winglets act like a barrier so the "nice" streamlines beneath and above are not disturbed, thus reducing the induced drag. There are variations to winglets in designs when it comes to the angle between the wing and winglet, height and aerodynamic body. Typical winglet designs are for example sharklets (Airbus A320), canted winglet (Boeing 747-400), raked wingtips (Boeing 767-400ER), and wingtip fence (Airbus A310).

2.3 Materials

When constructing aircraft, especially lightweight aircraft, the choice of material is important. The material needs to have low weight, yet a high stiffness relative to density to accomplish the low fuel consumption and stress resistance. Light metals, such as titanium, aluminum, and lithium alloy are commonly used in commercial aircraft and airframes (Aircraftcompare, 2019). When the idea of greener technology became more and more common, the use of composite materials grew. Carbon fiber reinforced polymer, or CFRP, is a composite material and is vastly used in the world of aviation. The composite offers a better strength-to-weight ratio than metals and is less sensitive to fatigue, due to its high Young's modulus and yield strength. The mechanical properties of this composite can be altered and customized to its purpose of use. The reinforcement fibers can be oriented in different directions and using different polymers as the matrix for optimizing stiffness and strength. In short, it's

lighter than aluminum and it is possible to modify the properties and allow fabrication of tapered or intricate sections, which makes the composite very applicable in commercial aircraft (Sastri, 2014).

Polyethylene is one of the easiest polymers to manufacture and has a wide range of applications. It is a polymer with great mechanical characteristics and is great for using as a film or as a skin [CES Edupack]. Polypropylene, like polyethylene, is one of the easiest polymers to manufacture as well. It is more rigid than the polyethylene but has lower strength and lower mechanical properties in general. Polypropylene can be referred to as the "younger brother" of polyethylene [CES Edupack].

Low-density polyethylene is a lighter version of polyethylene, with a good balance between flexibility and strength. The material has a wide combination of properties but still a good impact strength and excellent tear and stress crack resistance. Common areas of usage for LDPE are for example in electrical insulation or as a film material (Sastri, 2014).

Balsa wood is often used in wind turbine blades and sandwich structures as the material in-between, because of its very low density and high stiffness to density ratio (Casey, 2019). The lightweight wood is also often used in surfboards and model airplanes. Balsa wood is generally the lightest and softest of all commercial woods, ranging from 128.150 to 224.260 kg/m3. Despite its softness, it is technically classified as a hardwood. Therefore is cannot hold nails or screws very well, but gluing is the method of preference when working with this material. Balsa also has very good sound, heat, and vibration insulating properties (Wood-database, 2009).

Implementation

3.1 Working process

When a structure has been determined for examination, CAD programs such as Solid Edge ST10, ANSYS Spaceclaim, and Siemens NX were used to virtually construct the structure. A 3D model was already given by the supervisor; what needed to be done was integrating the chosen design of the wing structure. The next step was to compute preliminary relevant fluid and solid mechanics calculations and estimations. These were acquired via CFD simulation programs such as ANSYS Fluent and STAR CCM+. The solid mechanics of the wing was analyzed with FEM simulations using the built-in features in Solid Edge called FEMAP and another built-in FEM feature in Siemens NX.

To begin with the calculations, the loads on the UAV (self-weight included) needed to be determined. Hence, CFD-simulations were required to be computed first with the specifications applied. To find the materials that would fit the requirements for the UAV, CES Edupack was used together with material tables from different websites. CES Edupack is a database that offers a high variety of materials with their newly updated properties. With the completed design, the loads from CFD simulations, and a preliminary material of choice applied, a FEM-analysis was conducted to see if the wing could handle the stresses. These analyses were performed on the wing only, as they are the components that generate the majority of the lift. This procedure was repeated with a few materials for different angles of attack, to test which of the chosen materials would show the best results. After this step, the design was optimized to look at structures with different measurements that would yield the best results to meet the requirements given. The aim is to find the structure that is the most lightweight, yet withstands the stresses that are acting upon it.

Results

4.1 The conceptual design

In this section, the resulting CAD model is presented from different angles. The resulting model consists of a simple honeycomb structure, filling the inside of the hollowed wing and a simple wing skin.

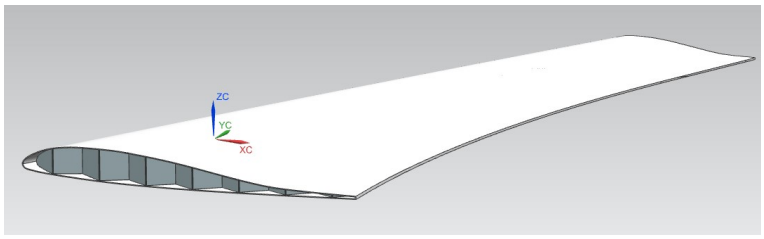

Figure 4.1: Right wing with honeycomb structure

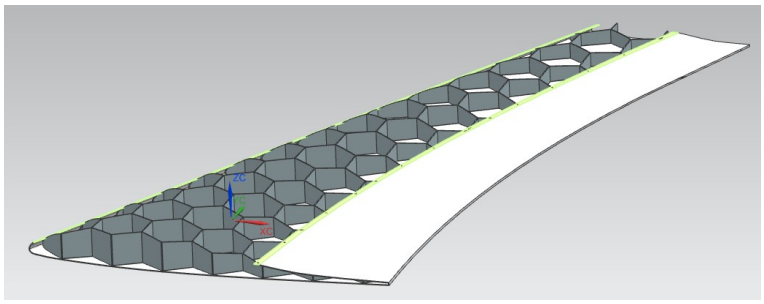

Figure 4.2: A section view of the right wing with honeycomb structure

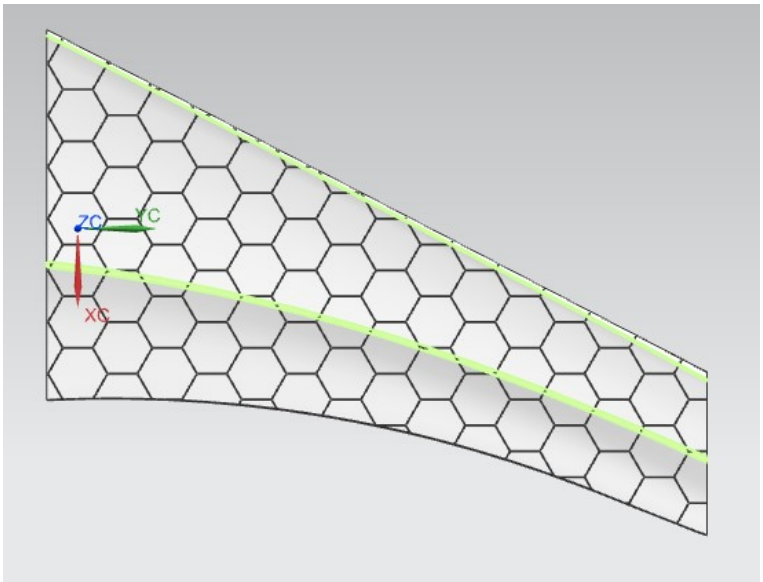

Figure 4.3: View from above showing how the honeycomb is placed inside the wing

The chosen design has a wing structure with a regular uniform skin with a thickness of 1mm, and a honeycomb structure inside that stretches throughout the whole inner volume, as shown in Figure 4.1. The honeycomb structure comprises hexagon structures with a diameter of 120mm (60mm as per the original, given design) and a wall thickness of 2mm (1mm as per the original, given design), which can be seen in Figure 4.2. The hexagons that compose the honeycomb structure have no space between one another, thus making the structure very rigid and stiff, as seen in Figure 4.3. The materials that were applied and tested on the honeycomb structure were the following: Balsa wood, polyethylene, polypropylene, and LDPE whilst on the wing skin, the same materials were applied and tested along with CFRP (with epoxy matrix).

4.2 Aerodynamic simulation

The results from the computational fluid dynamics simulations regarding the aerodynamic performance of the wing (in its original aerodynamic shape), are presented in this subsection. The simulations were made with the right-wing only.

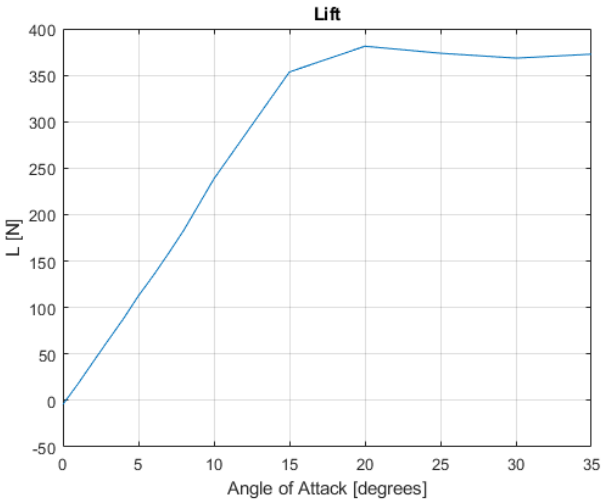

Figure 4.4: The lift force for a different angle of attack

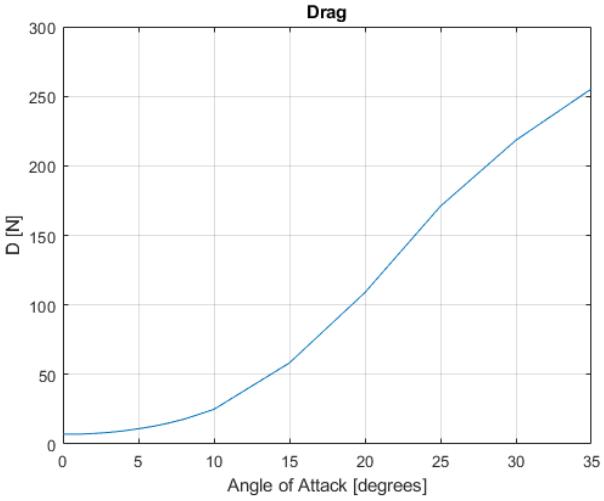

Figure 4.5: The drag force for different angle of attack

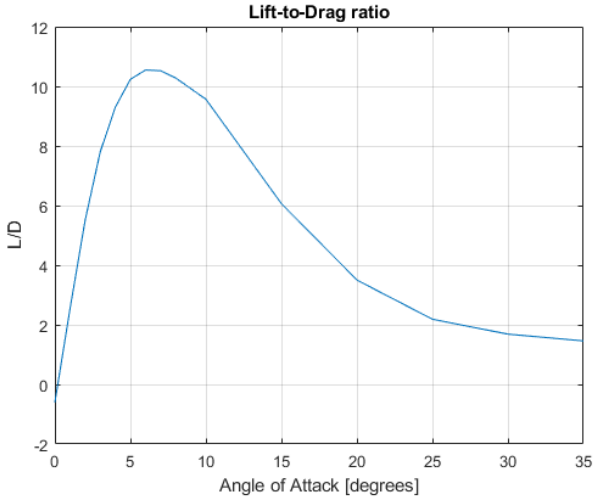

Figure 4.6: Lift to drag ratio (L/D) for different angle of attack

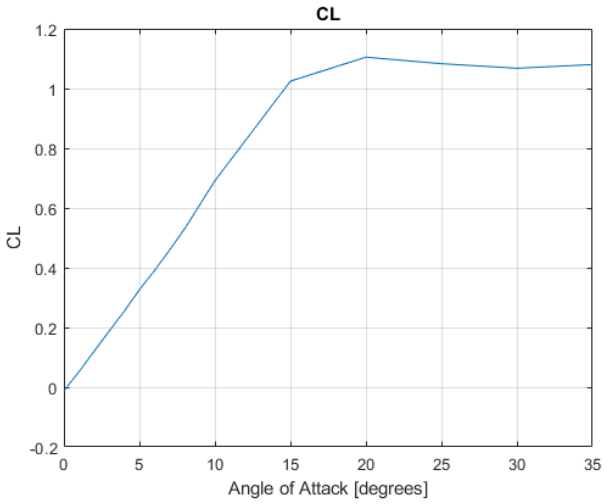

Figure 4.7: Lift coefficient for different angle of attack

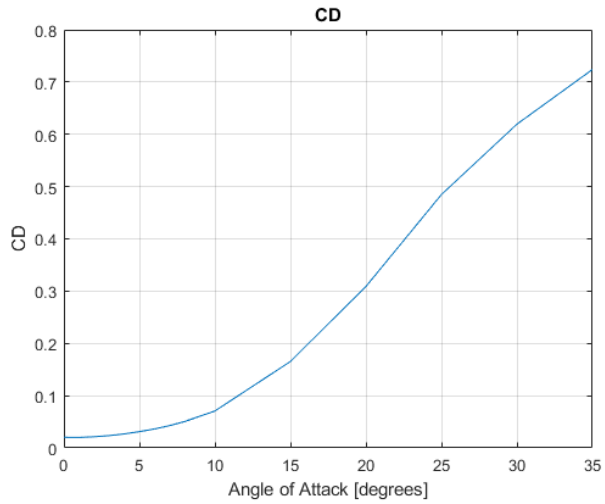

Figure 4.8: Drag coefficient for different angle of attack

Figure 4.4 to Figure 4.6 represents the lift and drag forces and the aerodynamic efficiency concerning the angles of attack. The lift and drag both increase to the angles of attack, as shown in Figure 4.4 and 4.5. However, the lift starts to decrease as it reaches higher angles, with a maximum lift of roughly 381.232N obtained at 20°, as shown in Figure 4.4. This is where stall occurs and the net lift distribution drops. The maximum lift-to-drag ratio of 10.547 occurs at 6°. The corresponding lift- and drag coefficients are presented in Figure 4.7 and Figure 4.8.

4.3 Stress analysis

The results from Tables 4.9 and 4.10 show the materials' mechanical characteristics and the stress analysis of the right-wing (only), simulated with the help of FEM.

Table 4.9 and Table 4.10 presents the material properties and the maximal von Mises stress acting upon the structure, for each material and material combination applied on the wing.

			Material		
Material properties	Balsa	CFRP (Epoxy matrix 50-50)	LDPE	Polypropylene	Polyethylene
Density [kg/mm^3]	1.60E-07	1.60E-06	9.10E-07	9.10E-07	9.60E-07
Young's Modulus [MPa]	300	1.50E+05	280	1.55E+03	896
Shear Modulus [MPa]	230	6.00E+04	225	548	314
Yield Strength [MPa]	6.9	1.05E+03	17.5	37.2	29
Tensile stength [MPa]	73	1.05E+03	10	41.4	44.8
Poisson's ratio	0.38	0.307		0.427	0.434

Table 4.9: Material properties

von Mises [MPa]	AoA(degrees)	1	2	3	6	20
Material combination, skin-honeycomb						
CFRP-Balsa (5.917kg)		-	-	-	2.994	-
CFRP-LDPE (6.569kg)		-		-	3.588	-
LDPE-Balsa (3.397kg)		1.267	0.620	3	4.590	15.680
Polyethylene-Balsa (3.397kg)		1.637	2.217	2.835	4.871	15.920
Polypropylene-Balsa (3.576kg)		0.671	0.340	1	4	14.880
Balsa-CFRP (2.087kg)		0.217	1.179	2	4.985	434.33
Balsa-LDPE (1.433kg)		0.224	1.210	2	5	15.270
Balsa-Polypropylene (1.480kg)		0.215	1.172	2.118	4.957	23.230
Balsa (Wing skin, 0.152kg)		1.341	3.540	5.717	12.260	35.920
Polyethylene (Wing skin, 3.246kg)		0.685	2.211	4.492	11.342	35.520
Polypropylene (Wing skin, 3.424kg)		0.626	2.104	4.192	10.463	10.014

Table 4.10: Maximal von Mises stress (Element-Nodal) [MPA]

Discussion

5.1 Approach

The working progress mentioned in section 3.1 was not fully followed due to many reasons such as complications of the given CAD model and the circumstances when considering the materials to be used. The method that was implemented was based on a systematic approach. Following this systematic approach made it easier to determine when to move on to the next step of the process. To choose the correct material combination, a FEM analysis had to be performed. To perform a FEM analysis and then find the stresses that act on the right-wing, a CFD simulation had to be done to find the external loads. To find the external loads, the CAD model had to be finished.

Due to the complexity of the wing structure, STAR CCM+ and Siemens NX was chosen for the simulations. These programs were selected for their ability to accurately handle the construction of the hexagonal structured core.

The materials that were chosen were mostly based on the literature review, but also based on the given requirements. Given the goal of a lightweight UAV, materials were chosen using CES Edupack. The optimal materials, given the weight constraint, were found to be plastics and composites.

The design that was implemented at the end was the honeycomb structure throughout the whole wing. This particular design was chosen because of its uniqueness and its rigid structure which entails strong mechanical properties, which is desired in the aerospace industry. Due to the walls of the hexagons connecting, the structure can handle the stresses well and since each hexagon is hollow, it can be considered as more lightweight. The honeycomb structure deviates from the traditional method of using ribs and spars, making it unusual but not unheard of.

5.2 Results

Results were acquired from the simulations at angles of attack between $1 - 3°$, because of the flight mode specification given for this project. When an aircraft is at cruising flight mode, the angle of attack will have a value between $0 - 3°$, as it does

for example Boeing 737 in cruise (Aviation StackExchange, 2014). The value for 0 however, was not tested due to the lift giving a negative value. Due to the angle of attack for the X8 Skywalker UAV in cruise being unknown, it was determined to examine all three angles and evaluating the stresses for these.

Eight different combinations of materials were used on the wing structure and each combination gave a different result. To begin with, two of the combinations, CFRP-Balsa and CFRP-LDPE weighed the most of all the combinations and were therefore not examined further. The other 6 combinations weighed around the same, so an optimal solution was deducted to be among them. Furthermore, the different stresses for each angle of attack can be seen in Table 4.9. The case for maximal lift (as well as the lift coefficient C_L seen in Figure 4.7) at an angle of attack of 20 degrees, was made to see if the combination could withstand higher stresses. Examining the same table, it is noticeable that three of the combinations with the balsa wood applied on the wing skin were the lightest combinations (about 2 kg or less). Since this project only considered the case where the UAV was cruising, the stresses at a lower angle of attacks were mainly focused on and considered acceptable. Out of the three combinations, balsa wood as the wing skin and low-density polyethylene (LDPE) as the honeycomb, weighed the least whilst still having stresses below the yield strength for each material (compare and see Table 4.10). Since the stresses were always far below the yield strength for each material, it did not matter whether the stresses were on the wing skin or the honeycomb structure.

Although balsa wood is very commonly used in many aerodynamic bodies, using it in the airframe might become a little tricky. Since wood is a natural material, balsa comes in numerous variations, causing a diversification of its mechanical properties. One common characteristic of the wood is its ease of absorbing water. This is not very desirable for an aircraft wing, even less so for a UAV that is to travel at an altitude of 2000m where it is exposed to rainwater and humid air. Due to this, the potential application of balsa wood as wing skin material was not developed further.

However, out of the material combinations that were tested for this project, polypropylene as wing skin and balsa as the interior honeycomb design, seemed the most compatible with the structural specifications and circumstances. Both materials attain the lowest stress values, for low as well as for high angles of attack. Additionally, this combination is very cost-efficient and has a reasonable weight at 3.58kg as shown in Table 4.9.

5.3 The Gurney flap

Designing of the trailing edge was attempted at the end of the project. A Gurney flap was mounted on the wing skin, along the trailing edge facing downwards. Different heights of the flap were tested: $1-3\%$ of the small chord (the cross-section nearest winglet) and 3% of the larger chord length (cross-section by the wing root) were analyzed (see Appendix A2). The purpose was to increase the lift-to-drag ratio but unfortunately, it did not do so. The lift at optimal lift-to-drag ratio (at $6°$) was increased to roughly $201N$ (see Appendix A.2 Figure A.2). However, as the lift increased, so did the drag force from a value of $12.775N$ to $25.767N$ for the same angle of attack. Since the lift force without the flap was around $134.727N$, which was considered acceptable together with no improvement of the lift-to-drag ratio, the flap was therefore unmounted and not continued with. A possible reason to why it did not contribute with much as desired, is the variable chord length of the wing. To find the perfect fraction of the several different cross-sectional chord lengths, would take a very long time and might be better off as a separate study in itself.

5.4 Error source

Many different simulation programs were used and all of them gave slightly different results. This could be due to their differences, e.g meshing methods, and numerical models for the iterative processes. Regarding meshing, Star CCM+ uses polyhedral meshes and has a problem adaptive cell convergence, and the user will not need to focus on this particular setting, whilst ANSYS Fluent uses a more open environment, which means the user needs to define cell sizes. To complete the numerical computations for the simulations, Star CCM+ uses Simpson's 1/3rd or 3/8th rule when solving, requiring more computational cost. Whilst ANSYS Fluent uses statistical iterative methods, such as the Newton-Raphson Iterative method, which are not as demanding as for Star CCM+ (Ismail, 2015).

As for the FEM simulations, based on experience from the early stages of this project, it was noticed that Solid Edge only used one core processor which yielded very slow simulations. Siemens NX however, can use more than one core allowing quicker and easier simulation. This was the main reason why it was decided to use Siemens NX instead of Solid Edge (Siemens Community, 2014).

CFD simulation

When setting up a CFD simulation, there are two different turbulence models to use: $k-\epsilon$ and $k-\omega$. The difference between these two models is how well they are applicable near boundary walls. The $k-\omega$ model is more sensitive to initial conditions and requires a longer processing time to reach acceptable residual values but the model will provide more accurate near-wall values. The $k-\epsilon$ model, on the other hand, requires less processing time and is not too sensitive to the initial conditions but is more common to use and easier to verify. The reason for choosing the $k-\omega$ turbulence model is because the lift-to-drag ratio is an important factor and since the drag force acts near the surface of the wing, $k-\omega$ would produce more accurate results (Argyropoulosa Markatosbc, 2014).

The number of iterations of the simulations affected computational efficiency. Therefore, it was the residuals during the CFD simulation that were the controlling parameters when the simulations should be stopped. It was decided that acceptable values for lift and drag were obtained when all of the residuals reached a magnitude of 10^{-4} or lower. Different programs use different models and methods when running their calculations, which should be taken into account when discussing the accuracy of the values calculated.

Mechanical properties

Much of the information acquired for balsa wood and LDPE were not fully accurate as they were taken from many websites which had a range of different values. To add on, the Poisson's ratio was not found for LDPE, thus making the simulations less accurate. Given that the material library in Siemens NX did not have the same values as CES Edupack, LDPE and balsa wood had to be added manually after searching the web. This affects the accuracy of the results as some of the properties of the materials were not found and some varied between websites. The properties were instead averaged to take these variations into account. The resulting material and their mechanical properties are seen in Table 4.9: polyethylene, polypropylene, and CFRP are taken from CES Edupack, whilst the other two were averaged and taken form the web.

A very important factor to keep in mind is that the usage of CFRP in this project is very simplified. The values used are for a carbon fiber composite with an epoxy matrix, 50% matrix, and 50% fiber, which are oriented in four directions (quasi-isotopic). These were directly taken from the CES Edupack database, without further calculations to optimize or customize the composite for this particular area

of application. This affects the general conclusion of this project, indicating that CFRP was not a suitable choice of material.

5.5 Applied materials

The materials that were examined in this project were all determined after the literature study. After doing some research on what lightweight materials were commonly used in the world of aviation but also in other wings, e.g in wind turbine blades, the most interesting and fitting ones were chosen. Since the real-life version is twice the size of the given CAD model, the weight and area had to be considered, given that the scaling would differ by a factor of 8 and 4 respectively. Since wood is used in wind turbine blades (3accorematerials, Accessed 2020), which are smaller than the wingspan of an aircraft, the idea of applying it on a UAV became an innovative idea.

5.6 Manufacturing and cost

The two polymers that have been used are similar as they are both made out of simple carbon monomers. Depending on the process techniques that are used, these materials' costs and characteristics can vary slightly. The cost for manufacturing polyethylene is roughly 14kg/SEK. The amount of polyethylene used on one of the models came up to about 3.246kg. For polypropylene, the cost for manufacturing is between 12,2-12,6kg/SEK, coming up to a weight of 3.424kg. The cost of manufacturing CFRP is between 306-339kg/SEK and weighing around 5.765kg, making it the most expensive material and dense out of the 5 chosen ones.

Balsa wood is considered to be very expensive due to the wood's natural variations, creating a hinder to the demand of the increasingly precise performance requirements for example in turbine blades (3accorematerials, Accessed 2020). The cost of the wood varies with the quality of the wood and the density. If a comparison is to be made, 1-ply of 2mm (3/32 inches) thick balsa sheet, which is the thickness of the honeycomb structure, will cost roughly 532,140 SEK/m^2 from the market (Specializedbalsa, Accessed 2020).

The price for LDPE resin in the UK is 301.213 SEK/kg and in Germany 890.946 SEK/kg. This means that if it were to be imported to and manufactured in Sweden, there would be transportation costs and CO_2 emission to take into account (Plasticsinsight, 2018).

5.7 Sustainable development and ethics

Out of all available polymers, polyethylene and polypropylene are made by processes that use the least amount of energy. Both of these polymers can be recycled and if they are contaminated, incineration is an option for retrieving the energy. This will be the same for LDPE since it is a variant of polyethylene. For CFRP, combusting the material can retrieve the energy back, otherwise placing it in landfills is the better option. These three materials are non-toxic as well. Balsa wood does not need fertilizers and grows relatively quickly. Developing a dedicating plantation will produce a good source for balsa wood, making it sustainable.

The main export of balsa wood comes from South American countries like Ecuador or Guatemala, which raises sustainability questions regarding local manufacturing, transportation costs, and CO_2 emissions. There is another alternative manufacturer of the balsa wood, the so-called Baltek® SBC balsa wood by 3A Composites Core Materials. They have FSC®-certified plantations situated in Ecuador and Papa New Guinea for their wood and they are also a supplier to aviation and wind turbine industries (3accorematerials, b).
Additionally, there seems to be a shortage of balsa wood on the market whilst the demand for precise performance is increasing. This has fueled new research to help the shortage, were mimicry of balsa wood with newly developed cellular composite materials, preserving the characteristics of lightweight and stiffness of the wood. This research is held by The Harvard School of Engineering and Applied Sciences and the Wyss Institute for Biologically Inspired Engineering. Their research is implying that these new materials will be able to mimic and improve balsa wood, and even the commercial 3D-printed polymers and polymer composites (Esler, 2014).

Conclusion

This study has shown that the new design with the honeycomb structure, in comparison to the UAV with a hollow wing, gave a significant improvement in handling the stresses. The wing skin should be made out of polypropylene, and the honeycomb from balsa wood, which gives a total weight of the right-wing of 3.576kg. The aerodynamic shape of the wing has remained the same because it received a good lift-to-drag ratio. The UAV with the current design will be able to fly with a cruising speed of 100 km/h at an altitude of 2000m (maximum condition), as results have shown.

6.1 Future work

To further develop this study, different dimensions of the honeycomb structure can be considered and tested. If the diameter of the honeycomb hexagons were to be increased, fewer materials would be applied and the weight could decrease even further. Alternative wing skin designs can also be further considered. The final wing skin structure resulted in a thickness of 2mm, which can be considered remarkably thin. Instead, incorporating the honeycomb structure within the skin or as the wing skin itself could become an interesting topic to study.

The material combinations of balsa as the wing skin could work if it was coated with a water-resistant material that could take higher stresses, such as a thinner layer of the polymers examined in this project or even a very thin layer of CRFP. This could potentially require more advanced FEM analysis, in which the volume of the materials could be modified and handled with percentiles or fractions of the CAD model. This would allow a more detailed calculation of the CFRP matrix-to-fiber distribution and the mechanical properties it would result in could be analyzed.

References

(3accorematerials, accessed 2020): 3accorematerials. *BALTEK® SB Selected grade structural balsa*. [www]. https://www.3accorematerials.com/en/products/baltek-balsa/baltek-sb-balsa. Published unknown. Accessed 18th of May 2020

(3accorematerials, accessed 2020): 3accorematerials. *BALTEK® SBC Plantation controlled structural Balsa for Infusion*. [www]. https://www.3accorematerials.com/en/products/baltek-balsa/baltek-sbc-balsa. Published unknown. Accessed 30th of April 2020

(Airbus, 2017): Airbus. *Composites: Airbus continues to shape the future*. [www]. https://www.airbus.com/newsroom/news/en/2017/08/composites--airbus-continues-to-shape-the-future.html. Published 1st of august 2017. Accessed 19th of March 2020

(Aircraftcompare, 2019): Aircraftcompare Editorial team. *9 Types of Aircraft Wings in Depth*. [www]. https://www.aircraftcompare.com/blog/types-of-aircraft-wings/. Published 4th of June 2019. Accessed 20th of January 2020

(Aircraftcompare, 2019): Aircraftcompare Editorial team.*What Materials Are Aircraft Made Of (Why) – Plane Design Priorities*. [www]. https://www.aircraftcompare.com/blog/what-are-planes-made-of/. Published 28th of November. Accessed 22nd of March 2020

(Aircraftsystemstech, accessed 2020): Aircraftsystemstech. *Wings - Aircraft Structures*. [www]. https://www.aircraftsystemstech.com/p/wings-wing-configurations-wings-are.html. Published unknown. Accessed 20th January 2020 (Allen, 2008): Allen, Bob. *Blended Wing Body – A potential new aircraft design*. [www]. https://www.nasa.gov/centers/langley/news/factsheets/FS-2003-11-81-LaRC.html. Last edited 22nd of April 2008. Accessed 18th of May 2020.

(Argyropoulosa Markatosbc, 2014): C.D.Argyropoulosa and N.C.Markatosbc. *Recent advances on the numerical modeling of turbulent flows*. [www]. https://www.sciencedirect.com/science/article/pii/S0307904X14003448. Published online 14th of July 2014. Accessed 21st of April

(Aviation StackExchange, 2014): Aviation StackExchange. *What is the wing angle of*

attack of a Boeing 737 in cruise?. [www]. https://aviation.stackexchange.com/questions/5150/what-is-the-wing-angle-of-attack-of-a-Boeing-737-in-cruise. Published 29th of May 2014. Accessed 30th of April 2020

(Aviation StackExchange, 2018): Aviation StackExchange. *How can I calculate the angle of attack of an airfoil?*. [www]. https://aviation.stackexchange.com/questions/47779/how-can-i-calculate-the-angle-of-attack-of-an-airfoil. Published 20th of January 2018. Accessed 30th of April 2020

(Boeing, 2017): Boeing. *VIDEO: 777X Folding Wingtip*. [www]. https://www.boeing.com/777x/reveal/video-777x-Folding-Wingtip/. Published 22nd of November 2017. Accessed 19th of March 2020

(Casey, 2019): Casey, Tina. *Absolute Beast Of A Wooden Wind Turbine Blade Rolls Off The Assembly Line*. [www]. https://cleantechnica.com/2019/04/19/absolute-beast-of-a-wooden-wind-turbine-blade-rolls-off-the-assembly-line/. Published 19th of April 2019. Accessed 20th of April 2020

(Engineersedge, accessed 2020): Engineersedge. . [www]. https://www.engineersedge.com/physics/viscosity_of_air_dynamic_and_kinematic_14483.htm. Published unknown. Accessed 28th of May 2020.

(Esler, 2014): Esler, Bill. *Balsa Wood Substitute Developed for Wind Turbine Blades*. [www]. https://www.woodworkingnetwork.com/wood/lumber-data-trends/Balsa-Wood-Subsitute-Developed-for-WInd-Turbine-Blades-286518311.html. Published 21st of December 2014. Accessed 22nd of April 2020

(Gudmundsson, 2014): Gudmundsson, Snorri. *Gurney Flap*. [www]. https://www.sciencedirect.com/topics/engineering/gurney-flap. Published unknows date 2014. Accessed 3rd of April 2020

(Ismail, 2015): Ismail, Ahmad, (Research Gate). *Fluent vs Star-CCM+?*. [www]. https://www.researchgate.net/post/Fluent_vs_Star-CCM. Published the 6th of August. Accessed 18th of May 2020

(Jianyue, 2017): Xue, Jianyue. *How the aviation industry is lowering its carbon footprint*. [www]. https://www.eco-business.com/news/how-the-aviation-industry-is-lowering-its-carbon-footprint/. Published 18th of December 2017. Accessed 18th of May 2020.

(Nasa, 2015): Nasa editor Nancy Hall. *Aircraft rotations*. [www]. https://www.grc.

nasa.gov/www/k-12/airplane/rotations.html. Last edited 5th of May 2015. Accessed 17th of March 2020

(Nasa, 2015): Nasa editor Nancy Hall. *Relative velocities*. [www]. https://www.grc.nasa.gov/www/k-12/airplane/move.html. Last edited 5th of May 2015. Accessed 17th of March 2020

(Nasa, 2015): Nasa editor Nancy Hall. *Parts of airplane*. [www]. https://www.grc.nasa.gov/www/k-12/airplane/airplane.html. Last edited 5th of May 2015. Accessed 17th of March 2020

(Nasa, 2019): Nasa editor Nancy Hall. *Mach Number*. [www]. https://www.grc.nasa.gov/www/k-12/airplane/mach.html. Last edited on the 9th of October 2019. Accessed 18th of May 2020.

(Plasticsinsight, 2018): Plasticsinsight. *LDPE (Low-Density Polyethylene): Production, Price and its Properties*. [www]. https://www.plasticsinsight.com/resin-intelligence/resin-prices/ldpe/. Published 2nd January 2018. Accessed 30th of April 2020

(Physics StackExchange, 2013): Physics StackExchange. *Difference resultant aerodynamics force on an airfoil and a flat plate*. [www]. https://physics.stackexchange.com/questions/83432/difference-resultant-aerodynamics-force-on-an-airfoil-and-a-flat-plate. Published 4th of November 2013. Accessed 17th of March 2020

(Sastri, 2014): Sastri, Vinny R. *Low Density Poly-Ethylene*. [www]. https://www.sciencedirect.com/topics/engineering/low-density-poly-ethylene. Published in 2014. Accessed 22nd of March 2020

(Siemens Community, 2014): Siemens Community. *When will Solid Edge start using multiple Cores*. [www]. https://community.sw.siemens.com/s/question/0D54O000061xL9PSAU/when-will-solid-edge-start-using-multiple-cores. Published 24th of December 2014. Accessed 18th of May 2020

(Specializedbalsa, Accessed 2020): Specializedbalsa. *Balsa Plywood Panels*. [www]. http://www.specializedbalsa.com/products/balsa_plywood.php. Published unknown. Accessed 30th of April 2020

(Teresko, 2007): Teresko, John. *Boeing 787: A Matter of Materials – Special Report: Anatomy of a Supply Chain*. [www]. https://www.industryweek.com/leadership/companies-executives/article/21942033/boeing-787-a-matter-of-materials-special-report-anatomy-of-a-supply-chain. Published 15th November 2007. Accessed 20th

March 2020

(Wood-database, 2009): Wood-database. *Balsa*. [www]. https://www.wood-database.com/balsa/. Published 10t of April 2009. Accessed 25th of April

(Wilner, 2011): Wilner, Tamar. *Boeing 787 Dreamliner to Cut Fuel 20%*. [www]. https://www.environmentalleader.com/2011/09/boeing-787-dreamliner-to-cut-fuel-20/. Published 27th of September 2011. Accessed 20th of March 2020

Appendix

A.1 Terminology

Angle of attack	The angle between the direction of flight/airflow and the wing chord line (see picture down below)
Lift force	The component of the aerodynamic force that acts directly perpendicular to the flow direction on the aircraft
Drag force	The component of the aerodynamic force that is parallel but reversed to the flow direction that resists the aircraft.
Lift-to-drag ratio	The ratio/quotient between the lift coefficient and the drag coefficient. The ratio should be high enough indicating a good lift force and a small drag force.
Flow separation	When the boundary layer has detached from the surface of the aerodynamic body into a wake. This occurs at a high angle of attack.
Incompressible	Incompressible flow indicates very small density changes on the material, therefore an assumption can be made that the material has the same density throughout the flow.
Freestream	The air upstream of the object before the body has deflected, slowed down, or compressed the air is called free stream and is denoted with V_∞.

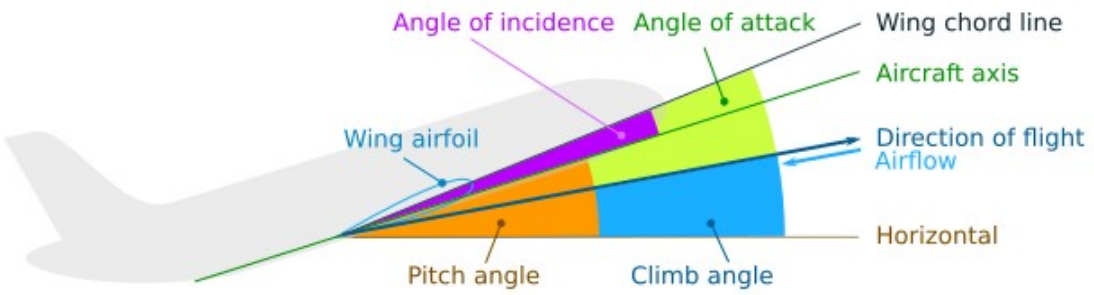

Figure A.1: Figure visualizing the relationship between the chord and diverse lines (Aviation stackexchange, 2018)

A.2 Aerodynamic simulation - Gurney flap

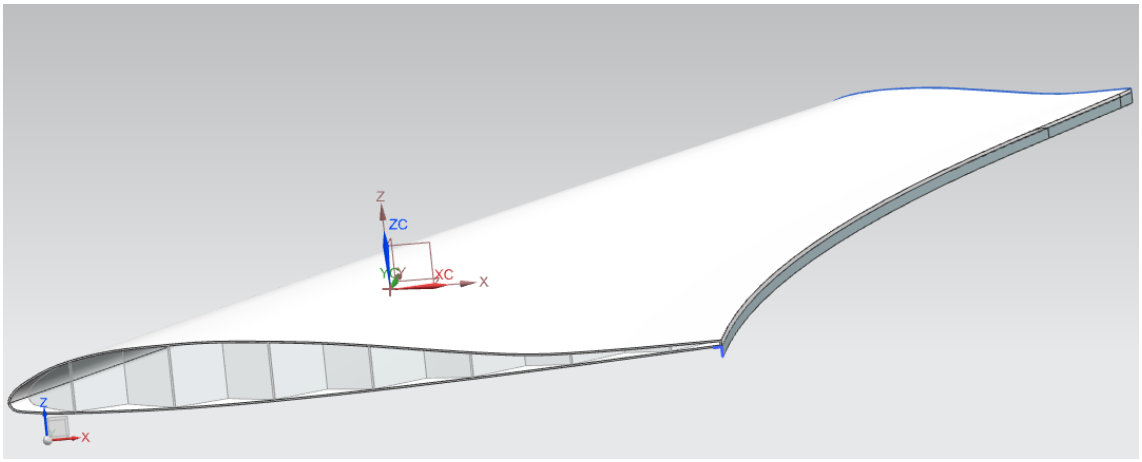

Figure A.2: Gurney flap mounted along the trailing edge

		Lift [N]	Drag [N]
Small chord	**1%**	162.601	17.954
	2%	131.284	13.221
	3%	151.088	16.203
Big chord	**3%**	201.684	25.767

Table A.3: Lift and drag force for different height of the Gurney flap. AoA = 5 degrees